Design of nano-modified PVDF matrices for lead-free piezocomposites: Small Graphene vs Carbon nanotube nano-additions

Jagdish A. Krishnaswamy[1], Federico C. Buroni[2], Enrique García-Macías[3] Roderick Melnik[1,4], Luis Rodriguez-Tembleque[4], Andres Saez[4]

[1]MS2Discovery Interdisciplinary Research Institute, Wilfrid Laurier University, 75 University Ave W, Waterloo, Ontario, Canada, N2L 3C5

[2]Department of Mechanical Engineering and Manufacturing, Universidad de Sevilla, Camino de los Descubrimientos s/n, Seville E-41092, Spain

[3]Department of Civil and Environmental Engineering, University of Perugia, Via G Duranti 93, Perugia 06125, Italy

[4]Department of Continuum Mechanics and Structural Analysis, Universidad de Sevilla, Camino de los Descubrimientos s/n, Seville E-41092, Spain

Abstract

Graphene nano-additions to polymer matrices have demonstrated exceedingly better mechanical properties compared to carbon-nanotube modified matrices. Therefore, in the context of mechanically superior high-performance piezo-composites, graphene-modified composite architectures represent an important design direction. In this paper, we first develop an effective property model for graphene-modified piezoelectric matrices, taking into account the mechanical anisotropy of the matrix. We further evaluate the piezoelectric performance of the matrix architecture which incorporates lead-free $BaTiO_3$ polycrystal inclusions. In order to obtain comparisons with well-established composites, we compare the electro-elastic response of two composite architectures in which the matrix is modified by multiwalled CNTs and graphene respectively. It is seen that, near percolation of the nano-additions, graphene-based systems exhibit an order of improvement in the piezoelectric response compared to the composite without nano-modification, an improvement similar to CNT-based systems, while exhibiting lesser than half the matrix-hardening observed in CNT-modified composites. This is due to a considerably smaller percolation threshold of graphene compared to CNTs which brings about percolative conditions at very small filler concentrations. Secondly, the electric fields produced within graphene-modified composites are smaller than in the case of CNT-modified composites. This is because of the higher permittivity of the matrix, in the case of the graphene-based design, at percolation. We also notice that the optimal inclusion polycrystallinity, at which the maximum electric flux is produced, is slightly smaller in the case of graphene-based designs and this optimum value increases with increasing inclusion concentrations, indicating that polycrystalline inclusions can be more effective in designs employing higher inclusion concentrations.

1. Introduction

Carbon nanotubes and graphene are important nanomaterials in the area of functionalized smart composites. This is because both the materials simultaneously exhibit excellent mechanical [1, 2] and electronic properties [3, 4], with extremely high Young's moduli (in the TPa range) as well as extremely high charge carrier mobilities (exceeding several 1000s of cm^2/Vs). Their ability to impart these properties to a matrix material has generated interest in the design of nanocomposites with excellent electro-mechanical properties. Although carbon nanotubes are well-understood and established as nanofillers for enhancing the elastic and electrical properties of nanocomposites,

graphene-based composites have been shown to exhibit exceedingly better mechanical behavior [5-7]. Owing to its relatively larger interfacial area and better adhesion to the matrix, graphene offers significant improvements in a range of mechanical properties including the Young's modulus [7], fracture strength [6], reduced crack propagation [6], and improved buckling resistance [5]. Further, graphene also improves the electrical conductivity of the matrix through the formation of percolative conductive networks of highly conductive graphene fragments [8]. Therefore, graphene modified polymer matrices are an important starting point in the design of functional nanocomposites which can exhibit significantly superior mechanical and electrical behavior.

In this paper, we compare the design of two nano-modified lead-free piezocomposites based on piezoelectric PVDF matrices. The designs include the modification of the PVDF matrix through addition of either multiwalled carbon nanotubes (MWCNTs) or graphene. We bring together our theoretical understanding of the effective elastic properties of CNT- and graphene-modified PVDF matrices and lead-free piezocomposite design using microscale polycrystalline $BaTiO_3$ inclusions. We first develop a model for the effective elastic properties of graphene-modified PVDF. This model takes into account the elastic anisotropy of PVDF. We further use these effective elastic coefficients in the design of lead-free piezocomposites with polycrystalline $BaTiO_3$ embedded in the nano-modified PVDF matrix. Further, we compare this composite design with the well-established CNT-modified piezocomposite design. Such a comparison leads to a better understanding of design contexts where using graphene as a nanofiller might be beneficial compared to CNTs. We observe major differences in the performance of these two variants of composite design because of the considerable differences in the elastic properties and dielectric (percolation parameters). The main aspects of comparison include the effective piezoelectric flux response, the electric field response, and the optimal polycrystallinity of inclusions leading to best performance.

2. Electro-elastic model and material property models

In this section, we provide details of the coupled electro-elastic model describing the piezoelectric response of the composites followed by the details of the material properties and models used in the simulations.

The composite architecture is modeled as a representative volume element (RVE) in two-dimensions ($x_1 - x_3$ plane). The geometry of the composite consists of randomly shaped lead-free microscale $BaTiO_3$ inclusions embedded in random positions within a square shaped matrix of sides a_m=b_m=50μm (Figure 1(a)). The matrix is modified with a uniform distribution of two types of non-agglomerated nanomaterials – (15,15) multiwalled carbon nanotubes (MWCNTs) and graphene. The phenomenological and governing balance equations describing the electro-elastic behaviour of the composites, respectively, are [9, 10]:

$$\sigma_{ij} = c_{ijkl}\varepsilon_{kl} - e_{kij}E_k,\ D_i = \epsilon_{ij}E_j + e_{ijk}\varepsilon_{jk}, \quad (1)$$

$$\sigma_{ij,j} = 0,\ D_{i,i} = 0, \quad (2)$$

where σ_{ij} and ε_{ij} are the stress and strain tensor components, respectively, and E_i and D_i are the components of the electric field and the electric flux density vectors, respectively. The material-dependent factors $c_{ijkl}, e_{ijk}, \epsilon_{ij}$ are the elastic, piezoelectric and the permittivity coefficients of the constituent materials of the composite. The relation between the strain and the displacement is

given by $\varepsilon_{ij} = \frac{1}{2}(u_{i,j} + u_{j,i})$. The implementation of the model in two-dimensions and the algorithms used to generate random polygonal inclusions can be found in [9]. The composite RVE is further subjected to two boundary conditions BC1 and BC2 as shown in Figure 1 (b)-(c), to obtain the effective piezoelectric coefficients e_{31} and e_{33}, respectively [9-12]. These coefficients represent the transverse and longitudinal piezoelectric response of the composite in two dimensions. The details of the RVE geometry investigated here are given in the appendix A1. The inclusions are geometrically modelled as a polygon with a random number of edges, *n*, chosen in the interval [10-20]. Further, the random vertices of the polygon are bounded within two concentric circles with random radii R1 and R2, which are selected in the ranges [2.5μm, 3.5μm] and [4 μm, 5 μm], respectively.

We next briefly discuss the material properties used in this investigation. The PVDF matrix and the $BaTiO_3$ inclusions are anisotropic in their electro-elastic behaviour. Further, the $BaTiO_3$ inclusions are assumed to be polycrystalline, the anisotropic properties of which are derived from the single crystal data as detailed in [9, 13]. Further, the matrix is modified by two types of nanofillers – (15,15) MWCNTs and graphene and the effective elastic properties of the matrix are obtained using the elastic properties of the nanofiller. The elastic coefficients of the PVDF matrix, $BaTiO_3$ single crystals, (15,15) MWCNTs, and graphene are presented in Table 1. For graphene, the Hill's moduli used for obtaining the transversely isotropic elastic coefficients are $(2k, l, n, 2m, 2p) = (1700, 6.8, 102\,000, 738, 204\,000)$ GPa [14, 15]. Table 2 further lists the dielectric and piezoelectric properties of the PVDF matrix and single crystal $BaTiO_3$.

Table 1: Elastic coefficients of PVDF (matrix), BaTiO3 single crystal (inclusions), (15,15) MWCNTs, and graphene (nanofillers)

Elastic coefficients (in GPa)	**Values for PVDF** [16]	**Values for $BaTiO_3$ (single crystal** [17]**)**	**Values for (15,15) MWCNT** [2]	**Values for graphene** [14, 15]
c_{11}	3.8	275.1	230.1	1219
c_{12}	1.9	178.9	211.9	481
c_{13}	1.0	151.55	66.3	6.8
c_{22}	3.2	275.1	230.1	1219
c_{23}	0.9	151.55	66.3	6.8
c_{33}	1.2	164.8	1429.9	102000
c_{44}	0.7	54.3	398	102000
c_{55}	0.9	54.3	398	102000
c_{66}	0.9	113.1	9.1	369

Table 2: The dielectric and piezoelectric properties of the matrix (PVDF) and inclusions ($BaTiO_3$)

Material property	**Values for $BaTiO_3$**	**Values for PVDF**
Relative permittivity		
ϵ_{11}/ϵ_0	1970 [17]	8 [16]
ϵ_{33}/ϵ_0	109	8
Piezoelectric coefficients (Cm^{-2})		
e_{15}	21.3 [17]	0 [16]

e_{31}	-2.69	0.024
e_{33}	3.65	-0.027

The effective elastic properties of the nano-modified PVDF matrices are obtained by using a classical Mori-Tanaka model which takes into account the anisotropic elastic coefficients of the matrix and the nanofiller, summarized in Table 1. Details of this methodology can be found in [18].

Nanofillers further modify the dielectric properties of the matrix [19]. The effective permittivity of the modified matrix has a percolative dependence on the nanofiller concentration given by [20]:

$$\epsilon_m^{eff} = \epsilon_m \left(\frac{f_c}{f_c - f_{nano}}\right)^p, \quad (3)$$

where ϵ_m and ϵ_m^{eff} are the permittivity of the pristine and the nano-modified matrices respectively, f_c and p are the percolation threshold and critical exponent which depend on both the nanofiller and the matrix, and f_{nano} is the concentration of the nanofiller in the matrix. Equation 3 implies a rapid increase in the effective permittivity of the modified matrix as the filler concentration f_{nano} approaches the percolation threshold f_c and the increase is more pronounced for higher values of the critical exponent p. We obtain the percolation parameters from experimental measurements on PVDF matrices with uniformly dispersed nanofillers. In the case of MWCNTs with an approximate aspect ratio of 100, f_c=1.14% and p=1.0068 [21]. In the case of graphene, the percolation threshold is much smaller, with f_c=0.18% and p=1.09 [22]. We emphasize here that adding more nanofiller to a matrix beyond the percolation threshold will lead to electrical shorting of the material and render it unusable and thus the percolation threshold is considered as the upper limit of nano-additions here. The piezoelectric response of the matrix is related to its β-phase content, which is influenced by the addition of nanofillers [23-25]. We note that this dependence is not completely characterized and the available data suggests a weak dependence which can be ignored considering much larger piezoelectric coefficients of the $BaTiO_3$ inclusions, and hence we model the piezoelectric coefficients of the matrix as constants given by the values of the pristine matrix.

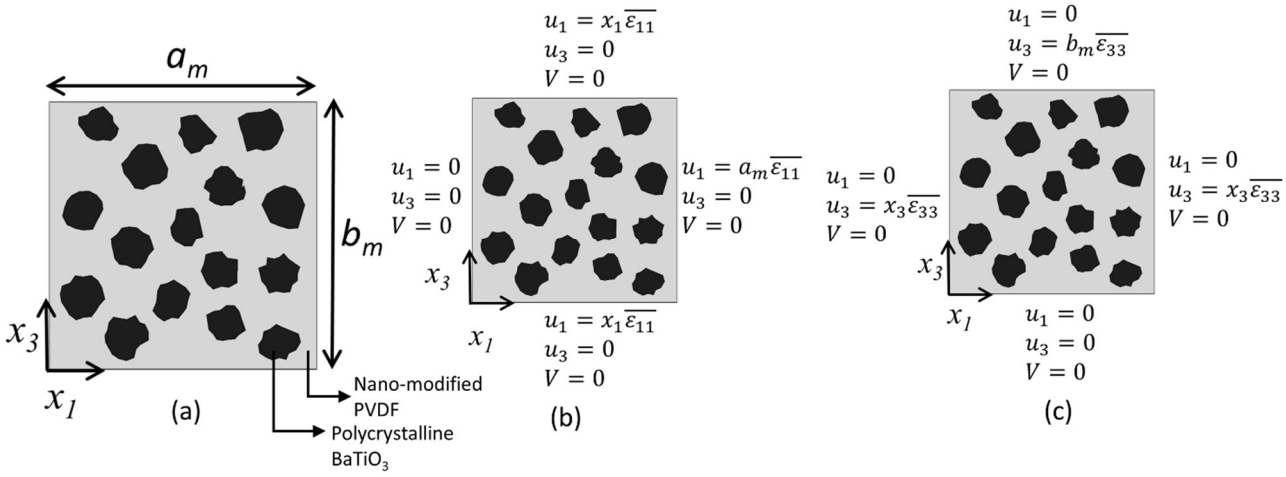

Figure 1 – (a) The schematic of the RVE investigated in this analysis with the coordinate system and the RVE dimensions, (b) and (c) are the boundary conditions BC1 and BC2, respectively, used to obtain the effective piezoelectric coefficients e_{31} and e_{33} respectively.

The polycrystallinity of the $BaTiO_3$ inclusions is an important design parameter. The effective electro-elastic properties of polycrystalline inclusions, the material model used to derive these quantities and the relevance of polycrystalline inclusions in piezocomposite design have been discussed elsewhere [9, 13]. The effective electro-elastic coefficients of polycrystalline inclusions are derived starting from the coefficients of $BaTiO_3$ single crystals [13]. The extent of polycrystallinity is quantified by using parameter α, such that $\alpha \to 0$ and $\alpha \to \infty$, respectively, correspond to the single crystalline and randomly oriented conditions. Values of α in between these extreme limits correspond to a controlled randomness with net orientation of grains along the poling direction (x_3 direction). The value of α depends on several factors including the crystal quality, poling conditions and so on [13].

3. Results and discussion

Although graphene leads to a significantly higher hardening of the matrix compared to a matrix modified by the same volume fraction of non-agglomerated nanotubes (see details in appendix A2), the graphene-based architecture has a much lesser percolation threshold. The implication of this is that adding more graphene to a percolated composite matrix will lead to electrical shorting and hence it is not possible in the context of a piezoelectric device. Therefore, when it comes to the maximum matrix hardening possible with a given nanomaterial, we are limited by the percolation threshold of the nanomaterial. Hence, we see that at percolation, the nanotube-modified matrices have around a 100% increase in the elastic coefficients, implying significant hardening. However, in the case of graphene, the increase is not so significant and is around a maximum of 50%. However, the permittivities of both matrices follow a percolative dependence on the volume fraction of the nanomaterial in the matrix. This means that near percolation conditions, the graphene-modified matrix is significantly softer than the CNT-modified matrix, while having similar significant improvements in the effective matrix permittivity. This is an advantage in the context of individually tailoring the mechanical and electrical properties of the composite. It is possible to significantly boost the permittivity while retaining the softness of the host matrix. In this particular case, it will be a considerable advantage, for example, in the design of wearable or flexible devices which can sense or harvest energy from mechanical stimuli. These devices require soft composites exhibiting appreciable electrical performance for which design strategies that allow boosting the electrical performance while not hardening the matrix further, are desired. It is also clear from Figures 2 (d)-(e) that both the CNT- and graphene- modified matrices lead to a percolative improvement in the piezoelectric response with a significant improvement near percolation (shown for a polycrystallinity index of α = 0.3, which is near the optimal value for best piezoelectric response). Based on this observation, all the analyses that follow are based on the behavior of the composite near percolation conditions, which is modeled as $f_{CNT} = 0.99 f_c$.

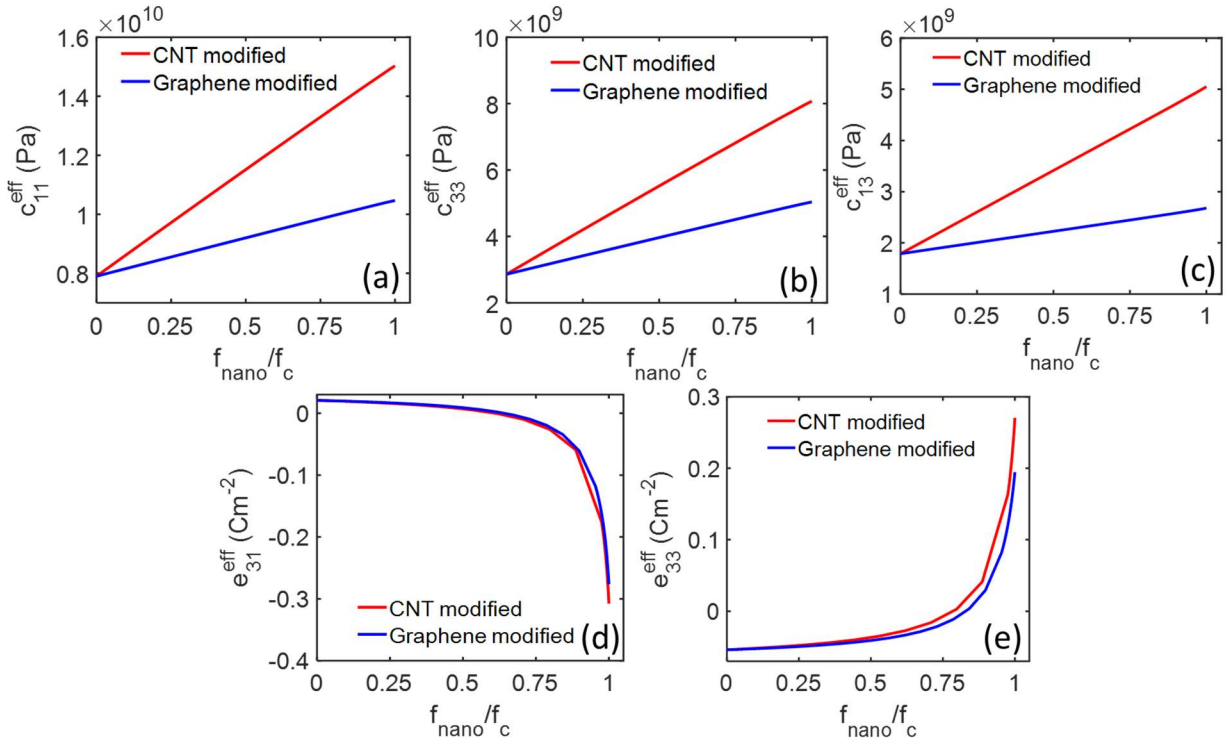

Figure 2 – (a)-(c) in sequence show the effective elastic coefficients c_{11}, c_{33}, and c_{13} of both nano-modified PVDF matrices as a function of the nanofiller concentration f_{nano} normalized by the percolation threshold f_c of the corresponding nanofiller. (d) and (e) show a percolative dependence of the effective piezoelectric coefficients e_{31} and e_{33} of the composite as a function of the normalized nanofiller concentration.

Figure 3 (a)-(c) and (d)-(f), respectively, show the effective piezoelectric coefficients e_{31} and e_{33} of the two composite architectures which are modified by CNTs and graphene. The results corresponding to very dilute $BaTiO_3$ loading are not presented here. This is because $BaTiO_3$ and PVDF have piezoelectric tensor coefficients (specifically, e_{31} and e_{33}) which are of opposite signs, owing to which, the addition of $BaTiO_3$ negates the piezoelectric activity of the PVDF and reduces the overall response of the composite for low $BaTiO_3$ concentrations. We have discussed this aspect earlier [18]. However, once the $BaTiO_3$ concentration exceeds a certain limit, the effective piezoelectric response of the matrix, especially in the presence of a percolated nano-modified matrix, is predominantly controlled by the $BaTiO_3$ inclusions with the matrix piezoelectricity contributing negligibly [18]. Accordingly, we see that in the case of both the nano-fillers, there is a significant increase in the piezoelectric response coefficients e_{31} and e_{33}. At higher inclusion concentrations, Figure 3 (b)-(f) indicate that an improvement of more than an order of magnitude is possible through graphene or CNT addition to the matrix. However, the piezoelectric response of graphene-based composites is still smaller compared to the CNT-based composites. This is mainly because of reduced matrix-hardening. Although graphene-based designs do not exceed the performance of CNT-based designs, an order of magnitude improvement in the piezoelectric response is still possible, compared to composites which are not nano-modified, while appreciably retaining the mechanical properties of the matrix. This observation is also in agreement with recent experimental work on graphene-modified PVDF/$BaTiO_3$ piezocomposites [26].

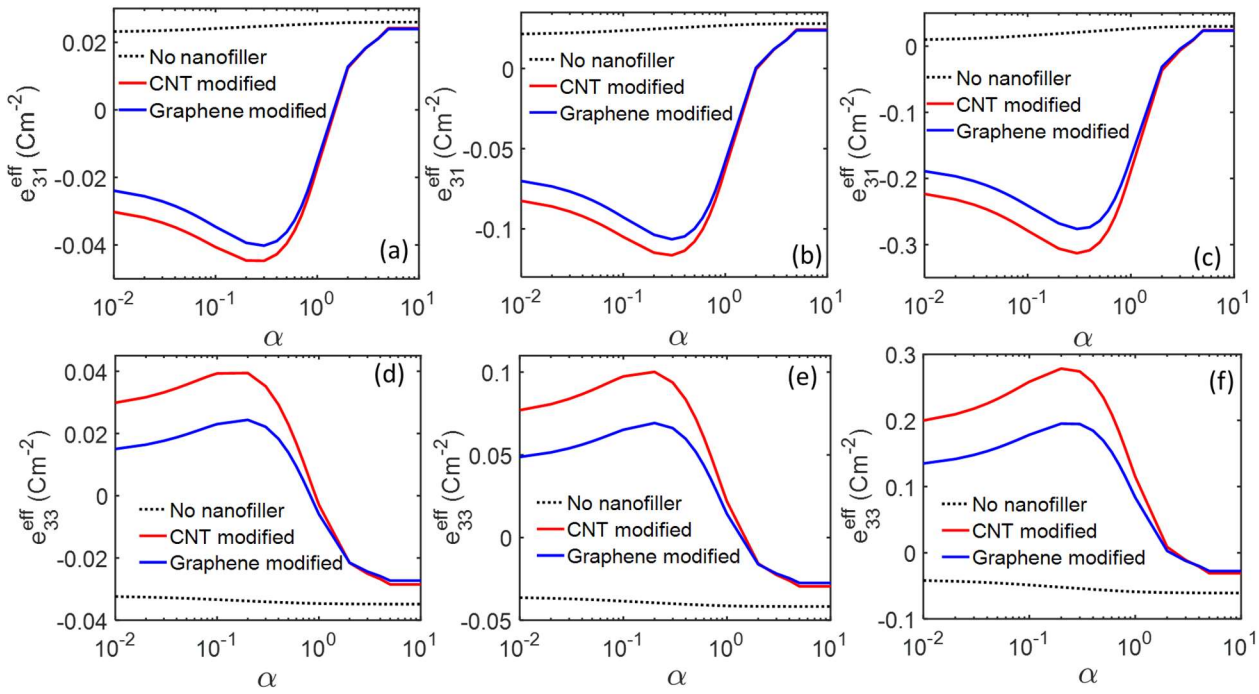

Figure 3 – The effective transverse and longitudinal piezoelectric coefficients, e_{31} and e_{33} respectively, of the nano-modified PVDF/$BaTiO_3$ composites for different $BaTiO_3$ inclusion concentrations V_{BTO} : (a) and (d) correspond to V_{BTO}= 14.7%, (b) and (e) correspond to V_{BTO}=25.9%, and (c) and (f) correspond to V_{BTO}=41.2%.

From Figure 3(a)-(f), it is also seen that the polycrystalline index α, at which optimum piezoelectric response results, is slightly different for CNTs and graphene. This could be due to a combination of the following factors – the difference in the elastic properties of the matrix at percolation and the difference in the permittivity of the matrix at percolation – which vary across the designs. Notably, although the graphene-modified PVDF matrix has much smaller elastic moduli compared to the CNT-modified matrices, the permittivity of the graphene-based system is relatively higher at percolation. From Equation 3, we understand that when $f_{CNT} = 0.99f_c$, the enhancement in the permittivity in graphene-modified PVDF is around 150 times of the pristine PVDF permittivity, while in the case of CNT-modified PVDF, the enhancement is around 100.

In Figure 4(a)-(b), we further plot the optimal α which leads to maximum piezoelectric flux generation (i.e. maximum e_{ij}) for both piezocomposite architectures (CNT-modified and graphene-modified), as a function of the volume fraction of the $BaTiO_3$ inclusions, V_{BTO}. First, we notice that the optimal polycrystalline index for graphene-modified systems is slightly higher consistently, for all V_{BTO}, compared to the CNT-modified system. Further, the optimal polycrystalline index increases with an increase in V_{BTO}. These results have the following implications: (a) graphene-nanomodifications can allow the use of slightly more polycrystalline piezoelectric inclusions for optimum performance and therefore allow more tolerances in the processing of high quality piezoelectric crystals, and (b) higher $BaTiO_3$ inclusion concentrations allow the introduction of higher polycrystallinity to maximize the piezoelectric response.

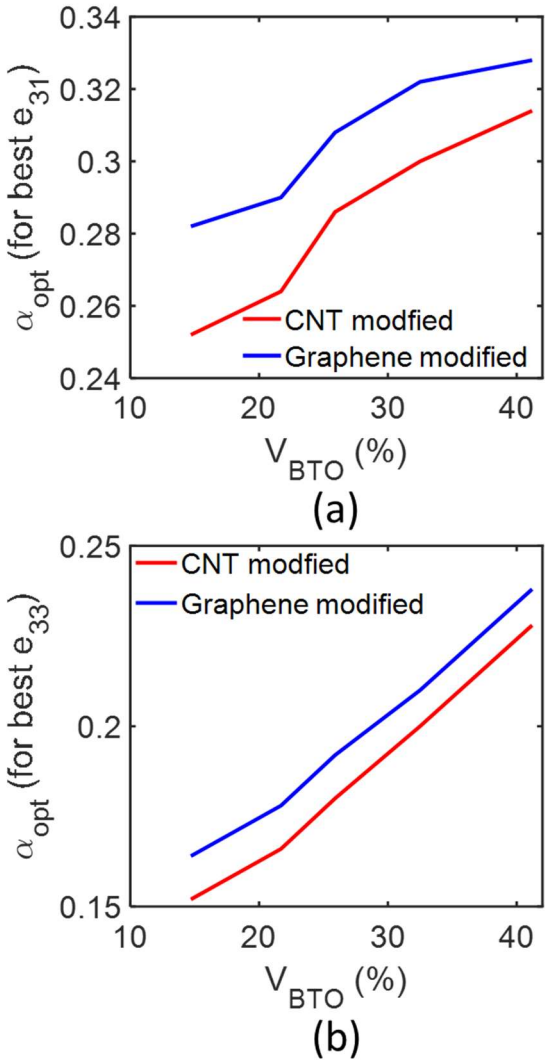

Figure 4 – the optimal polycrystallinity index α_{opt} for the best piezoelectric flux response of the composite. (a) corresponds to the best e_{31} and (b) corresponds to the best e_{33}.

We further point out that the effectiveness of a piezocomposite material is measured by its ability to simultaneously generate high electric flux and electric fields [27, 28]. In fact, the product of the piezoelectric flux coefficient and the field coefficient ($d_{ij}g_{ij}$) is a measure of the energy density in a piezocomposite. Usually, there is a tradeoff between the flux and field generating processes [27] and effective design needs to take into consideration a balance between these processes. In this context, we explore the electric field coefficient in the CNT- and graphene-modified composites, given by:

$$\xi_{ij} = \frac{\langle E_i \rangle}{\overline{\varepsilon_j}}, \tag{4}$$

where the numerator in the right-hand side is the volume averaged electric field, and the denominator is the applied boundary strain (refer to Figure 1(b)-(c)) in the Voigt notation. For example, ξ_{31} is the ratio of the volume averaged electric field generated in the x_3 direction normalized by the axial strain in the x_1 direction (i.e. $\overline{\varepsilon_{11}} = \overline{\varepsilon_1}$). Given the present two-dimensional

context, we will refer to ξ_{31} and ξ_{33} as the transverse and longitudinal electric field coefficients, respectively.

We present the transverse and longitudinal electric field coefficients, ξ_{31} (Figure 5(a)-(c)) and ξ_{33} (Figure 6(d)-(f)), respectively, for three different volume fractions. We note that the electric field generated in the graphene-based composite is smaller than in the case of the CNT-based composite, irrespective of the polycrystallinity index α. This is because of the higher permittivity of the graphene-modified PVDF matrix near percolation, as pointed out earlier, compared to the CNT-modified matrix. This increased permittivity is due to the differences in the percolation properties of CNTs and graphene, where particularly graphene has a slightly larger critical exponent which gives larger permittivity enhancements due to the percolative effect. It is thus evident that an optimal critical exponent p is necessary to obtain a permittivity which is high enough to obtain a large permittivity to support the flow of electric flux from the high-permittivity inclusion environment through the surrounding matrix. However, it should be low enough to ensure that the electric fields within the composite do not get compromised. The critical exponent, as seen from experimental literature on CNT-based composites [29], is tunable through chemical functionalization of the nanotubes. One can envisage such an atomic/molecular level design even for graphene-based composites to further tune the critical exponent to an optimal value. Also, the dependence of the electric field response on the polycrystallinity and the existence of an optimal α for maximum electric field generation gradually fades out at higher inclusion concentrations, unlike in the case of the electric flux response where clear local maxima exist even at higher inclusion concentrations.

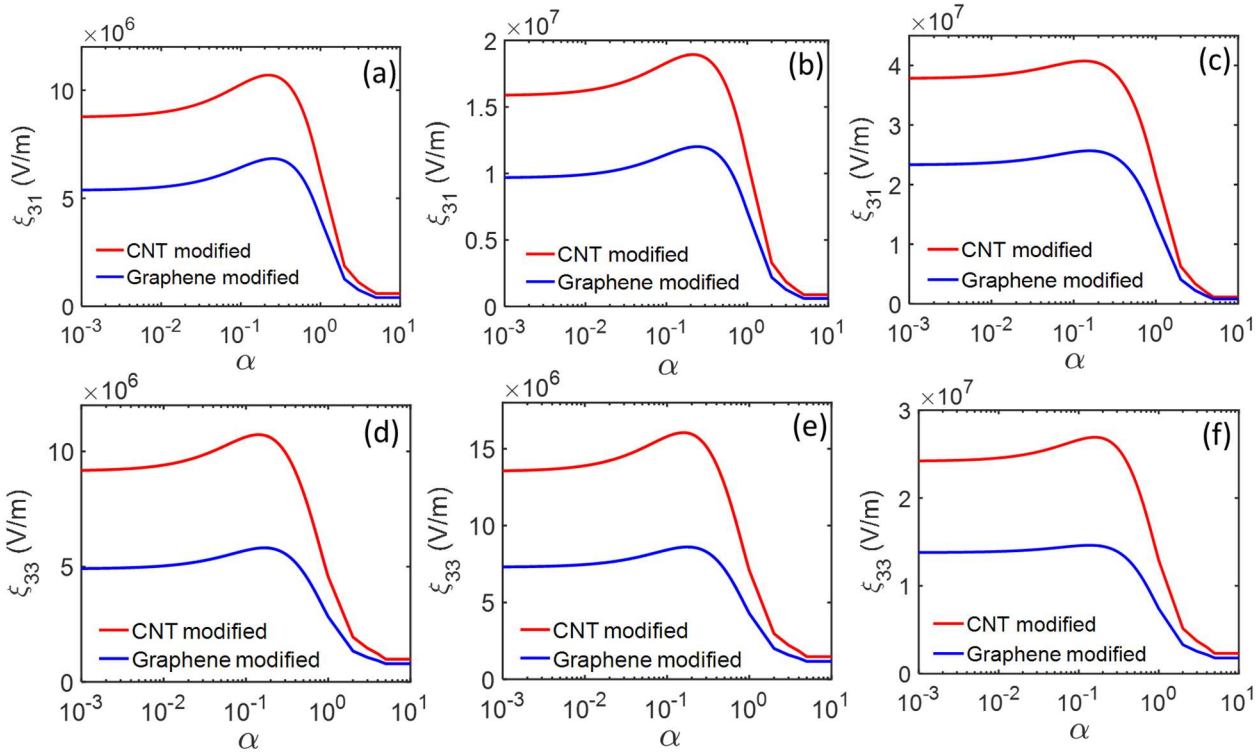

Figure 5 – the volume averaged electric field normalized by the applied strain, for different volume fractions. (a)-(c) correspond to the transverse response ξ_{31} and (d)-(f) correspond to the

longitudinal response ξ_{33}. As in Figure 3, (a) and (d), (b) and (e), and (c) and (f) correspond to V_{BTO}=14.7%, 25.9%, and 41.2%, respectively.

In summary, we have observed that significant enhancements (an order of magnitude) in the electric flux generation are possible in both CNT and graphene-modified PVDF matrices. However, in contrast to CNT-modified composites, the considerably smaller percolation threshold in the case of graphene can allow such improvements in flux generation without significant matrix hardening. Secondly, the higher permittivity of graphene-modified composite at percolation results in reduced electric field generation compared to CNT-modified composites. Thirdly, we have noticed that the optimal inclusion polycrystallinity leading to maximum flux generation, at percolation, is slightly higher in the case of the graphene-based composite and this optimal value increases with increasing inclusion concentration indicating that polycrystal-based designs could be more useful in composites with larger inclusion concentrations. From the perspective of design, this means that a larger quantity of inexpensive of microscale polycrystals can lead to a better design compared to high-quality single-crystal inclusions.

4. Conclusions

We have explored the design of nano-modified PVDF-based lead-free piezocomposites by developing a new effective property model accounting for the elastic anisotropy in PVDF. Using this modeling approach, we have compared the performance of piezocomposites modified by carbon-nanotubes and graphene. While CNT addition is a well understood route to boost piezoresponse, graphene holds more promise in terms of better mechanical properties of the modified matrix. Firstly, in terms of piezoelectric response, although the graphene-based design results in lesser electric flux generation compared to the CNT-based design, it can still lead to an order of magnitude improvement near percolative conditions compared to composites which are not nano-modified. Secondly, with increasing inclusion concentrations, the optimal inclusion-polycrystallinity for maximum flux generation also increases, thus pointing to the fact that using larger quantities of polycrystalline materials could lead to optimum performance and practically viable solutions to superior piezoelectric performance. Thirdly, graphene-based designs generate smaller electric fields compared to CNT-based designs because of higher matrix permittivity at percolation. Lastly, the graphene-modified composites require piezoelectric inclusions of slightly higher polycrystallinity, compared to CNT-modified composites, for optimum flux generation. This indicates that using graphene as a nano-modifier allows for slightly more process intolerances in the processing of high quality of piezo-crystals, which would directly impact the cost of their production. Also, in both the composite systems, the optimum polycrystallinity for best flux generation at percolation of the nanofiller, increases as the piezoelectric inclusion concentration is increased. This further suggests that using larger quantities of relatively more polycrystalline piezo-crystals might be an interesting route to maximize piezo-response in a scalable manner. In conclusion, we note that graphene-modified piezocomposites provide improvements similar to CNT-modified systems, while allowing for higher inclusion polycrystallinity and better retention of the matrix elasticity. This makes graphene a viable alternative to CNTs especially in application requiring flexible high-performance piezocomposites.

References

[1] Ovid'Ko I 2013 Mechanical properties of graphene *Rev. Adv. Mater. Sci* **34** 1-11

[2] Shen L and Li J 2005 Transversely isotropic elastic properties of multiwalled carbon nanotubes *Physical Review B* **71** 035412

[3] Bolotin K I, Sikes K J, Jiang Z, Klima M, Fudenberg G, Hone J, Kim P and Stormer H L 2008 Ultrahigh electron mobility in suspended graphene *Solid State Communications* **146** 351-5

[4] Dürkop T, Getty S, Cobas E and Fuhrer M 2004 Extraordinary mobility in semiconducting carbon nanotubes *Nano letters* **4** 35-9

[5] Rafiee M, Rafiee J, Yu Z-Z and Koratkar N 2009 Buckling resistant graphene nanocomposites *Applied Physics Letters* **95** 223103

[6] Rafiee M A, Rafiee J, Srivastava I, Wang Z, Song H, Yu Z Z and Koratkar N 2010 Fracture and fatigue in graphene nanocomposites *small* **6** 179-83

[7] Rafiee M A, Rafiee J, Wang Z, Song H, Yu Z-Z and Koratkar N 2009 Enhanced mechanical properties of nanocomposites at low graphene content *ACS nano* **3** 3884-90

[8] Kim H, Abdala A A and Macosko C W 2010 Graphene/polymer nanocomposites *Macromolecules* **43** 6515-30

[9] Krishnaswamy J A, Buroni F C, Garcia-Sanchez F, Melnik R, Rodriguez-Tembleque L and Saez A 2019 Improving the performance of lead-free piezoelectric composites by using polycrystalline inclusions and tuning the dielectric matrix environment *Smart Materials and Structures* **28** 075032

[10] Saputra A A, Sladek V, Sladek J and Song C 2018 Micromechanics determination of effective material coefficients of cement-based piezoelectric ceramic composites *Journal of Intelligent Material Systems and Structures* **29** 845-62

[11] Qin R-S, Xiao Y and Lan H 2014 Numerical simulation of effective properties of 3d piezoelectric composites *Journal of Engineering* **2014**

[12] Sladek J, Sladek V, Krahulec S and Song C 2016 Micromechanics determination of effective properties of voided magnetoelectroelastic materials *Computational Materials Science* **116** 103-12

[13] Li J Y 2000 The effective electroelastic moduli of textured piezoelectric polycrystalline aggregates *Journal of the Mechanics and Physics of Solids* **48** 529-52

[14] Ji X-Y, Cao Y-P and Feng X-Q 2010 Micromechanics prediction of the effective elastic moduli of graphene sheet-reinforced polymer nanocomposites *Modelling and Simulation in Materials Science and Engineering* **18** 045005

[15] Garcia-Macias E, Rodriguez-Tembleque L and Saez A 2018 Bending and free vibration analysis of functionally graded graphene vs. carbon nanotube reinforced composite plates *Composite Structures* **186** 123-38

[16] Odegard G M 2004 Constitutive modeling of piezoelectric polymer composites *Acta materialia* **52** 5315-30

[17] Berlincourt D and Jaffe H 1958 Elastic and piezoelectric coefficients of single-crystal barium titanate *Physical Review* **111** 143

[18] Krishnaswamy J A, Buroni F C, Garcia-Macias E, Melnik R V N, Tembleque L-R and Saez A Design of lead-free PVDF/CNT/BaTiO3 piezocomposites for sensing and energy harvesting: The role of polycrystallinity, nanoadditives, and anisotropy (submitted)

[19] Gaiser P, Binz J, Gompf B, Berrier A and Dressel M 2015 Tuning the dielectric properties of metallic-nanoparticle/elastomer composites by strain *Nanoscale* **7** 4566-71

[20] Pecharroman C, Esteban-Betegon F, Bartolome J F, Lopez-Esteban S and Moya J S 2001 New Percolative BaTiO3–Ni Composites with a High and Frequency-Independent Dielectric Constant (ϵr≈ 80000) *Advanced Materials* **13** 1541-4

[21] Yao S-H, Dang Z-M, Jiang M-J, Xu H-P and Bai J 2007 Influence of aspect ratio of carbon nanotube on percolation threshold in ferroelectric polymer nanocomposite *Applied physics letters* **91** 212901
[22] Fan P, Wang L, Yang J, Chen F and Zhong M 2012 Graphene/poly (vinylidene fluoride) composites with high dielectric constant and low percolation threshold *Nanotechnology* **23** 365702
[23] Huang L, Lu C, Wang F and Wang L 2014 Preparation of PVDF/graphene ferroelectric composite films by in situ reduction with hydrobromic acids and their properties *RSC Advances* **4** 45220-9
[24] Kim G H, Hong S M and Seo Y 2009 Piezoelectric properties of poly (vinylidene fluoride) and carbon nanotube blends: β-phase development *Physical chemistry chemical physics* **11** 10506-12
[25] Lee J S, Kim G H, Kim W N, Oh K H, Kim H T, Hwang S S and Hong S M 2008 Crystal structure and ferroelectric properties of poly (vinylidene fluoride)-carbon nano tube nanocomposite film *Molecular Crystals and Liquid Crystals* **491** 247-54
[26] Shi K, Sun B, Huang X and Jiang P 2018 Synergistic effect of graphene nanosheet and BaTiO3 nanoparticles on performance enhancement of electrospun PVDF nanofiber mat for flexible piezoelectric nanogenerators *Nano Energy* **52** 153-62
[27] Maurya D, Peddigari M, Kang M-G, Geng L D, Sharpes N, Annapureddy V, Palneedi H, Sriramdas R, Yan Y and Song H-C 2018 Lead-free piezoelectric materials and composites for high power density energy harvesting *Journal of Materials Research* **33** 2235-63
[28] Priya S 2010 Criterion for material selection in design of bulk piezoelectric energy harvesters *IEEE transactions on ultrasonics, ferroelectrics, and frequency control* **57** 2610-2
[29] Li Q, Xue Q, Hao L, Gao X and Zheng Q 2008 Large dielectric constant of the chemically functionalized carbon nanotube/polymer composites *Composites Science and Technology* **68** 2290-6

Appendices

A1: Details of the RVE geometries

The RVEs investigated here with the inclusion volume fraction V_{BTO} are shown in Figure AF1 (a)-(e).

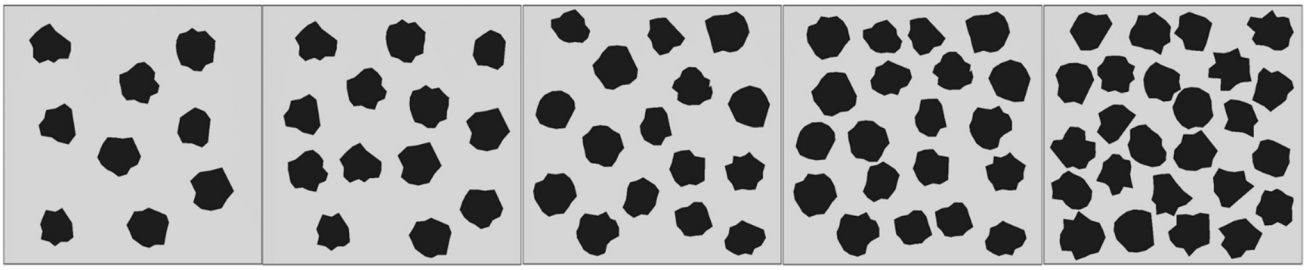

Figure AF1 – The RVEs investigated in this analysis with different inclusion volume fractions, V_{BTO}.

A2: Effective elastic coefficients of nano-modified PVDF

Figure AF2 shows the effective elastic coefficients, relevant to the two-dimensional analysis carried out here. Graphene has a significantly larger (>50%) hardening effect compared to CNTs. However, at percolation, due to much smaller percolation thresholds in the case of graphene, the

matrix hardening is considerably lesser than the CNT-modified PVDF, as would be seen from Figure 2.

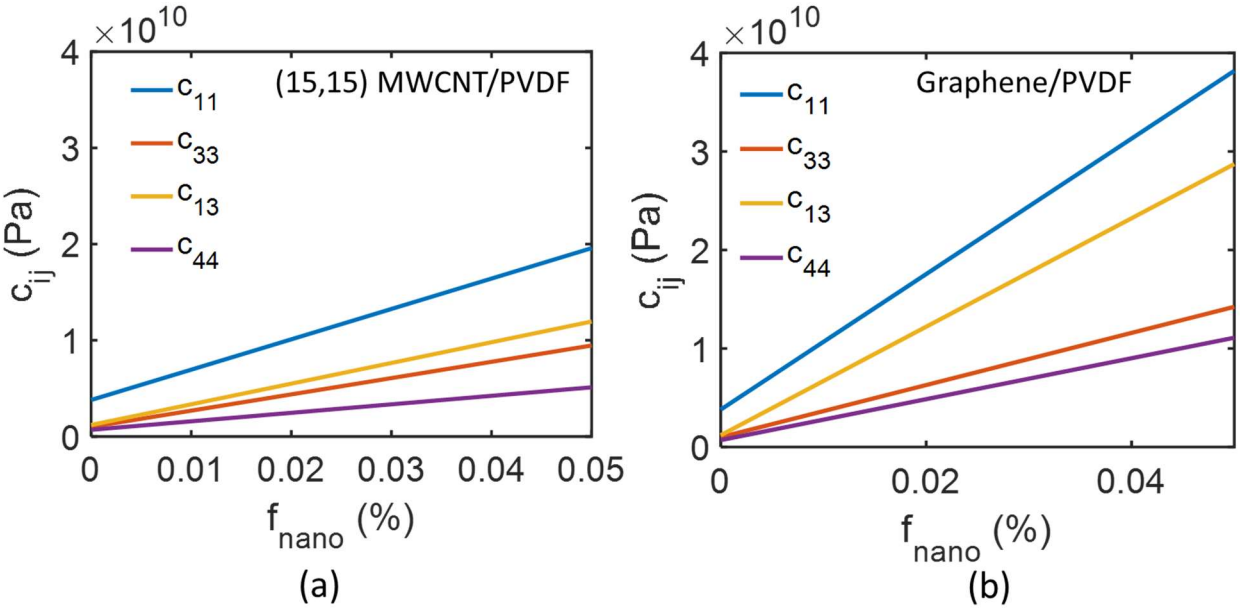

Figure AF2 – Effective elastic coefficients of (a) CNT-modified PVDF and (b) Graphene-modified PVDF, as a function of the nanofiller concentration f_{nano}